# Shrub Dieback in a Semiarid Ecosystem: The Integration of Remote Sensing and Geographic Information Systems for Detecting Vegetation Change

*Kevin P. Price**
Department of Geography and Kansas Applied Remote Sensing (KARS), University of Kansas, Lawrence, KS 66045
*David A. Pyke*
Department of Range Science and the Ecology Center, Utah State University, Logan, UT 84322-5230
*Lloyd Mendes*
Department of Range Science, Utah State University, Logan, UT 84322-5230

ABSTRACT: During several years of high precipitation (1982-84) in the Great Basin region of the western U.S., many plant communities showed evidence of shrub dieback, primarily of shadscale (*Atriplex confertifolia*). The potential relationship between dieback and climatic change suggested the need for an objective test of the usefulness of remotely sensed data in detecting vegetation changes in a semiarid ecosystem.

Two techniques were evaluated for their effectiveness in predicting shrub dieback. In the first technique, an unsupervised classification of Landsat Thematic Mapper (TM) data was used to predict the distribution of dieback. Spectral reflectance patterns associated with dieback were identified using a goodness-of-fit test. In the second technique, pre- and post-dieback Multispectral Scanner (MSS) data and change detection analyses were used to predict dieback distribution. The accuracy of both prediction techniques was tested against field verified data using an index of association.

The unsupervised classification technique correctly predicted shrub dieback and nondieback in better than 70 percent of the locations. The results suggest that spectral classes from an unsupervised approach can be associated with natural environments that are most susceptible to shrub dieback. Results from the change detection technique showed that infrared reflectance from known dieback areas averaged 9.8 brightness values lower than areas of nondieback. However, agreement between the change detection map and field verified data indicates that the prediction map was not significantly better than a random classification. The findings of this study provide additional information related to exotic annual weed invasion dynamics in a Great Basin semiarid shrub environment.

## INTRODUCTION

REGARDLESS OF WHETHER CHANGES IN VEGETATION CHARACTERISTICS are a result of climatic changes, pathogen or herbivore outbreaks, or by alterations in land-use practices, improved mapping and monitoring methods are needed that enable detection and assessment of environmental conditions and trends. The methodologies for detecting subtle environmental changes over broad geographic areas are largely undeveloped. Many monitoring strategies rely on either subjective observations or on small sample plots (e.g., rangeland trend plots). With recent concerns about the impact of climatic changes on plant communities around the world, remotely sensed data have been proposed as a means to monitor geosphere and biosphere dynamics (Tueller, 1987; Woodwell *et al.*, 1984; Rasool, 1985; NASA, 1988). Satellite imagery has been used for a variety of environmental studies such as determining above-ground plant biomass (Maxwell, 1976; Tucker, 1979), estimating leaf area (Wiegand *et al.*, 1979; Running *et al.*, 1986), and mapping vegetation (Bauer *et al.*, 1979; Hoffer, 1984; McGraw and Tueller, 1983; Mueller-Dombois, 1984; Price *et al.*, 1985; Tucker *et al.*, 1985; Wilson and Tueller, 1987). Large scale changes in the landscape have been monitored using multitemporal satellite imagery to create change detection maps (Robinove *et al.*, 1981; Carneggie *et al.*, 1983; Pilon *et al.*, 1988).

In most cases, efforts to monitor vegetation change with remotely sensed spectral data have been limited to vegetation communities that show abrupt changes in physiognomy and spectral characteristics. These have been mainly forest and desert systems monitored for deforestation and desertification (Woodwell *et al.*, 1984; Woodwell *et al.*, 1987; Mann *et al.*, 1984; Robinove *et al.*, 1981). Environmental impacts that result in the reduction or elimination of selected plant species allow one to test the sensitivity and utility of remotely sensed data for monitoring subtle environmental changes. Before global monitoring and assessment efforts are initiated, the usefulness of remotely sensed data to detect changes in plant composition should be explored in arid/semiarid environments where vegetation is often sparse (< 30 percent cover) and plant species composition is diverse. Such environments present unique challenges for remote sensing, both from a scientific and from a management viewpoint (Tueller, 1987).

A constraint in using satellite digital imagery for environmental monitoring is that changes must dominate a large enough area to influence the reflectivity of multiple pixels. Areas with dieback of natural vegetation often meet this criterion. Dieback usually affects only a few species distributed over large geographic areas. While a few studies have used satellite images for detecting and monitoring large scale vegetation dieback (Rock *et al.*, 1986; Vogelmann and Rock, 1988), none of these studies have examined dieback in semiarid shrublands.

A recent dieback of shrubs in the Great Basin is suspected to have begun after 1982. Within Utah, over 400,000 ha of land with high shrub mortality were reported by the Bureau of Land Management (K. Boyer, personal communication, 1984). Nearly half of the affected area was located within shrub-steppe eco-

*Much of the research was completed while in the Department of Geography at Utah State University, Logan, UT 84322

PHOTOGRAMMETRIC ENGINEERING & REMOTE SENSING,
Vol. 58, No. 4, April 1992, pp. 455–463.

0099-1112/92/5804–455$03.00/0

systems of the Great Basin. The affected species included big sagebrush (*Artemisia tridentata* Nutt.), bud sage (*Artemisia spinescens* Eat.), shadscale (*Atriplex confertifolia* (Torr. & Frem.) S. Wats.), fourwing saltbush (*Atriplex canescens* (Pursh) Nutt.), and winterfat (*Ceratoides lanata* (Pursh) J.T. Howell). Above average precipitation from 1982 to 1984 is suspected to be related to dieback (Nelson *et al.*, 1989; Pyke and Dobrowolski, 1989), suggesting that this phenomena might be stimulated by climatic changes.

## STUDY AREA

Puddle Valley, located 96 km west of Salt Lake City, Utah, is a partially drained desert basin bounded by the Grassy Mountains to the west and the Lakeside Mountains to the east. The valley runs north to south for approximately 24 km and is about 13 km wide. The entire study area was located approximately within the boundaries of the U.S. Geological Survey (USGS) 7.5-minute Puddle Valley, Utah quadrangle (Figures 1a and 1b). Precipitation at the site comes mainly during the winter as snow. The closest weather station in Tooele, Utah (approximately 50 km away) reports the total annual precipitation to be 412 mm.

The predominant vegetation is shadscale, green molly (*Kochia americana* Wats.), greasewood (*Sarcobatus vermiculatus* (Hook.) Torr.), and cheatgrass (*Bromus tectorum* L). Dieback was apparent within the valley between the playa bottom, at 1300 m in elevation, and the edge of the valley basin, at 1600 m in elevation. The density of pre-dieback shadscale (i.e., before 1982) was estimated to be between 3000 and 5000 individuals/ha by counting both live and dead plants in 1987. In areas of severe dieback where the live-to-dead shrub ratio is 1:5, exotic annuals such as belvedere summer cypress (*Kochia scoparia* (L.) Schrad.), halogeton (*Halogeton glomeratus* Meyer.), and cheatgrass were often abundant (Ewing and Dobrowolski, 1991).

## METHODS

Two digital image analysis techniques were used to test the accuracy of remotely sensed data for predicting the distribution of shrub dieback. In the first technique, a Thematic Mapper (TM) image was classified using a clustering algorithm and minimum-distance-to-mean classifier. In the second technique, change detection maps were created using multitemporal Landsat Multispectral Scanner (MSS) imagery acquired for three different years.

Similar image restoration and preprocessing methodologies were applied to the TM and MSS imagery. The histogram minimum method (Chavez, 1975) was used to standardize image pixel brightness values (BV) to account for varying physical characteristics of the atmosphere at the time of image acquisition. Image restoration for line striping was performed using a mean and standard deviation correction technique (Rohde *et al.*, 1978). The output prediction maps were geographically rectified to a Universal Transverse Mercator (UTM) projection using a nearest-neighbor resampling operation (Jensen, 1986). For overlay purposes, the pixel size for all maps produced from MSS data was resampled to a common size of 30 m by 30 m to match the cell size of the verification map. This resampling approach is commonly used when lower resolution images are compared to higher resolution images (Iverson and Risser, 1987; Jakubauskas *et al.*, 1990; Walker and Zenone, 1988; Sader, 1987). All image

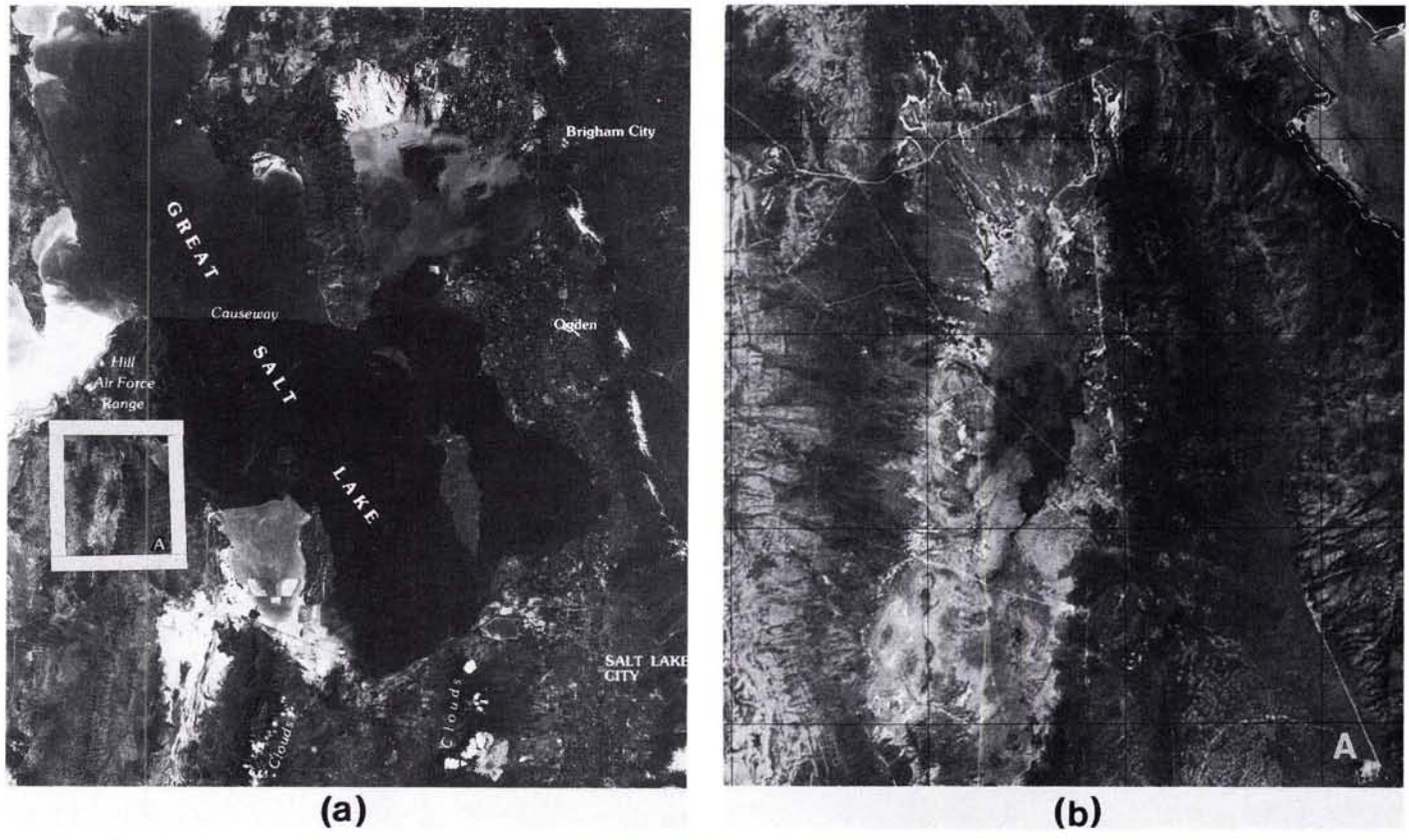


FIG. 1. (a) Great Salt Lake and vicinity with Puddle Valley study area outlined by a white rectangle. (b) Enlargement of the Puddle Valley study area. The back "comma" shaped pattern surrounded by lighter tones in the middle of the figure is the Puddle Valley playa. The ground distance is 5000 metres between the black graticules superimposed on the image. (Figures were photographed from the Great Salt Lake and Vicinity poster, U.S. Geological Survey, 1984.)

processing and geographic information systems (GIS) analyses were performed using the Earth Resources Data Analysis System (ERDAS Inc., Atlanta, Georgia).

### Unsupervised Classification Approach

A mid-spring TM image, 24 May 1987, was selected to coincide with peak growth and greenness in the study area (Price *et al.*, 1985). On the raw TM image, 18 consecutive bad lines were removed from the lower middle half of the image. The image was preprocessed as described previously and the Tasseled Cap universal coefficients (Crist and Cicone, 1984; Kauth and Thomas, 1976) were used to transform the TM digital values to produce brightness, greenness, and wetness components. This transformation was used in an attempt to enhance the spectral reflectance of the sparse desert vegetation.

Untransformed TM data were also used to predict shrub dieback, but to conserve computer storage space and decrease processing time, the analyses were performed using the red (0.63 to 0.69 μm), near infrared (0.76 to 0.90 μm) and the two middle infrared (1.55 to 1.75 μm and 2.08 to 2.35 μm) bands (TM bands 3, 4, 5, and 7). The blue-green (0.45 to 0.52 μm) and green (0.52 to 0.60 μm) bands were omitted because they contributed little additional information due to high band intercorrelation (blue-green versus red, $r = 0.945$ and green versus red, $r = 0.805$). The thermal (10.4 to 12.5 μm) band was also omitted because emittance measurements throughout the study area showed minimal variation and the spatial resolution of the thermal band is poor, relative to the other bands.

Both the transformed and untransformed TM images were classified separately into 75 spectral classes using an unsupervised clustering algorithm and a minimum-distance-to-mean classifier. The 75 spectral classes for each image were associated with land-cover types located in the field. Because dead shrubs can be found in nearly every shrub community, including healthy communities, a field site was classified as dieback if greater than 95 percent of the shrubs within a 90-m by 90-m (3- by 3-pixel area) vicinity were dead. The threshold of 95 percent was used because, on most sites, the shrubs were either all dead, or mostly alive. The percent dieback at each site was visually estimated.

During the summer of 1988, a survey to locate dieback areas was conducted along roadways traversing the study area. The use of roadways as reference features made it possible to more accurately identify dieback locations on the USGS Puddle Valley orthophotoquadrangle. Dieback sites encountered along the road were selected only if they were away from disturbed areas of the roadway and less than 135 m from the center of the road (e.g., 9-pixel wide buffer zone, 270 m wide, with 1 pixel covering the road right-of-way and 4 pixels, 120 m wide, on each side of the road). In addition, one transect was walked along an east- west section fence to map dieback across the study area and away from roadways. Along this transect, all dieback within 75 m of either side of the fence was mapped (e.g., a 5-pixel buffer, 150 m wide). The 135-m and 75-m distances were used because it was estimated that these were the maximum distances at which dieback could be positively identified from the truck and on foot. Along both the road and fence transects, dieback areas smaller than 90 by 90 m (3 by 3 pixels) were ignored to minimize the inclusion of bordering hybrid pixels. Polygon boundaries around dieback areas were drawn well within the affected sites to ensure nondieback areas were not included in the polygons. Because all dieback areas within the 270-m and 150-m buffer zone could be observed and mapped, the resulting map constitutes a comprehensive survey of all dieback within the buffer zone.

The polygon boundaries for the known dieback areas were digitized and converted to a raster format for manipulation and analysis in a GIS. The buffer zones along the transects were created by digitizing the UTM coordinates of the roads and fence and using a GIS search operation to locate all pixels within the specified buffer distance. A GIS map overlay operation was used to merge the identified dieback locations and the buffer zone into a new map that showed areas within the buffer distance that were classified during the road survey as either dieback or nondieback (Figure 2).

Using GIS map overlay and cross-tabulation operations, the observed frequency of the 75 spectral classes within known dieback areas of the buffer zone was calculated for both the transformed and untransformed images. A spectral class was defined as a dieback class if its observed pixel frequency, within known dieback areas, was significantly greater than a random pixel distribution of the class. An example of observed and expected pixel frequencies used in the analysis is given in Table 1. The null hypothesis was that within the buffer zone the pixel frequencies for each spectral class within dieback areas would not differ significantly from pixel frequencies within areas of nondieback. The hypothesis was tested using a log likelihood ratio Chi-square test of independence between dieback categories and spectral classes (G-test, Sokal and Rohlf, 1981) ($P \leq 0.01$). This technique is similar to the approach used by Lowell and Astroth (1989). Spectral classes with low expected frequencies of occurrence ($< 5$) were combined so that the analysis was not biased (Sokal and Rohlf, 1981). Spectral classes with observed frequencies of zero in either dieback or nondieback areas, but not in both, were considered important structural zeros in the analysis; thus they were set to $10^{-6}$ because the analysis technique must take the logarithm of the observed frequency (log(0)

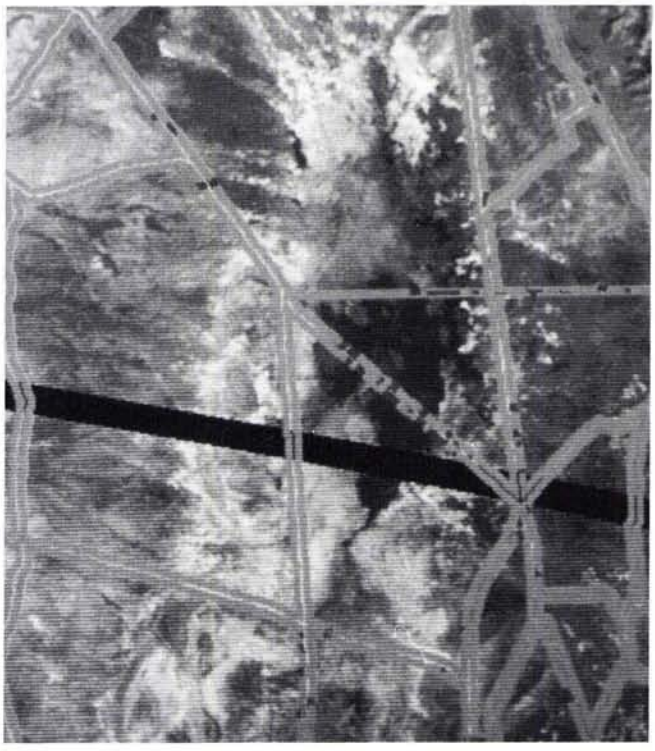

FIG. 2. Classification map (75 classes) of Puddle Valley study area showing the results of the unsupervised classification of transformed TM imagery. The light gray strips represent the 270-m and 150-m buffer zones for known locations of nondieback. The dark gray areas within the light gray buffer zone represents locations of known shrub dieback. The pixel class frequencies within the buffer zone were used to determine which of the 75 spectral classes were associated with dieback. The wide diagonal black strip crossing the map is where 18 bad lines of the image were deleted from the original TM data.

TABLE 1. A SAMPLE OF THE OBSERVED AND EXPECTED PIXEL FREQUENCIES USED IN THE GOODNESS-OF-FIT TEST TO ASSOCIATE SPECTRAL CLASSES WITH SHRUB DIEBACK. THE "OBSERVED FREQUENCY" REPRESENTS THE NUMBER OF CLASS PIXELS COINCIDING WITH AREAS OF KNOWN DIEBACK. THE "EXPECTED FREQUENCY" REPRESENTS THE NUMBER OF CLASS PIXELS EXPECTED TO COINCIDE WITH AREAS OF DIEBACK IF THE PIXELS WERE DISTRIBUTED RANDOMLY. CLASSES WITH POSITIVE OBSERVED DIFFERENCES (OBSERVED − EXPECTED) WERE TESTED AGAINST A CHI-SQUARE CRITICAL VALUE AT 1 D.F. AND P = 0.001. CLASSES WITH SIGNIFICANT POSITIVE VALUES WERE CLASSIFIED AS DIEBACK.

| Spectral Class | Observed Pixel Frequency | Expected Pixel Frequency |
|---|---|---|
| **1*** | **145** | **70** |
| 2 | 0 | 34 |
| 3 | 17 | 67 |
| **4*** | **53** | **45** |
| 5 | 0 | 11 |
| 6 | 7 | 44 |
| 7 | 0 | 3 |
| 8 | 21 | 43 |
| 9 | 0 | 28 |
| 10 | 12 | 57 |
| 11 | 7 | 25 |
| **12*** | **155** | **65** |
| 13 | 7 | 23 |
| 14 | 12 | 61 |
| 15 | 26 | 44 |
| 16 | 0 | 1 |
| 17 | 0 | 15 |
| 18 | 22 | 56 |
| 19 | 38 | 67 |
| 20 | 0 | 5 |

*Spectral classes that were predicted to be associated with dieback because the difference between their observed and expected frequencies was positive and exceeded the Chi-square critical value.

is undefined). Spectral classes with observed frequencies of zero in both areas were not analyzed because they did not contribute to the predictability of dieback.

If pixel frequencies for spectral classes were found to be associated significantly with dieback areas, then each class with a positive residual (i.e., an affinity with dieback) was tested to determine the individual classes that significantly contributed to the overall G-statistic. This was done by comparing the calculated G-statistic for the spectral class to a Chi-squared critical value at 1 d.f. and P = 0.001. This technique for determining the individual classes associated with dieback was not used as a statistical test, but as a nonbiased means of identifying classes likely to be associated with areas of dieback. Using this technique, it was determined that, for the transformed image, 6 of 75 and for the untransformed image, 6 of 75 spectral classes were observed in dieback areas more frequently than expected if the spectral classes had been randomly distributed.

Based on the results of the G-statistic, two shrub dieback prediction maps (one from transformed, one from untransformed data) were created by recoding each of the 75 spectral classes to either dieback or nondieback. The accuracy of the prediction maps was tested against field verified data that were collected independent of, and not used as, the field site data described in the previous section. Areas qualifying as field verification sites were homogeneous in vegetation appearance and in dieback status over at least a 90- by 90-m (3- by 3-pixel) area. The verification sites were located along other roadway and linear features (jeep roads, telephone lines, etc.) not traversed during the initial roadway survey. The UTM coordinates and vegetation condition (dead or alive) of each verification site were digitally encoded, converted to a raster format, and saved as a GIS map layer. A GIS search operation was used to create an output map with a 3- by 3-pixel buffer around the location of each verification site. The verification map was registered to the dieback prediction maps and an overlay operation was used to extract, from the dieback map, the pixel class values that corresponded to the 3- by 3-pixel verification sites. To avoid the influence of hybrid pixels upon the accuracy estimates, field verification sites were eliminated if their location corresponded to nonhomogeneous 3- by 3-pixel groups extracted from the dieback prediction maps.

The two dieback prediction maps were compared to the retained field verification sites, and a likelihood ratio Chi-square (G) was used to test independence among predicted and observed occurrences of dieback and nondieback (SAS Institute Inc., 1988). Significant ($P < 0.05$) values of G indicated that prediction maps and field verification data were significantly associated. The Goodman-Kruskal Gamma ($\gamma$) was used to determine the strength and the direction (positive versus negative) of the associations (Liebetrau, 1983; SAS Institute Inc., 1988). ($\gamma$ may range from $+1$ indicating absolute agreement, to $-1$, indicating absolute disagreement, with 0 indicating no association between predicted and observed dieback and nondieback classes.)

### CHANGE DETECTION APPROACH

Two change detection maps were created using MSS imagery from three different dates: 13 May 1975, 19 May 1979, and 10 May 1988. These images were collected by Landsats 1, 3, and 5, respectively. The selection of the three images was based on the following criteria: (1) availability of high-quality satellite imagery with minimal cloud coverage, (2) coverage of the study area before and after the presumed dates of shrub dieback (between 1982 and 1986), (3) similarity in annual precipitation patterns, and (4) coincidence with the peak vegetation growth period of the area.

A change detection map was created for the pre-dieback period (prior to 1982) by subtracting the image brightness values for the near-infrared channel (0.7 to 0.8 μm) of the 1975 image from that of the 1979 image (1979 *minus* 1975). The post-dieback change detection map (after 1982) was created by subtracting the brightness values for the same channel of the 1979 image from that of 1988 (1988 *minus* 1979). A near-infrared, as opposed to a visible band, was selected for the analysis because of its increased sensitivity to vegetation conditions. The second infrared channel (0.8 to 1.1 μm) was not used in the change detection analysis because the 1975 image was missing this channel. To avoid the calculation of negative difference values, the output values were recoded to numbers ranging from 0 to 255, and a value of 127 was assigned to areas where there was no change in the IR reflectivity. A value greater than 127 would indicate higher reflectance in the later image and a value less than 127 would indicate higher reflectance in the earlier image (Jensen, 1986).

The same dieback and nondieback locations within the roadway buffer zone and the field verification sites were also used to analyze and assess accuracy of the prediction results produced by the change detection approach. The use of areas within the buffer zone, with known ground conditions as control sites, allowed discrimination of spectral variation due to sensor differences among MSS scanners, atmospheric attenuations and large-area environmental/climatic differences, from variation due to vegetation change. Theoretically, spectral variation unrelated to dieback would probably affect areas of dieback and nondieback equally.

A distribution map of predicted dieback was developed from change detection results if the mean difference values for areas of known dieback differed significantly ($P < 0.05$) from the mean difference values for areas of nondieback within the buffer zone. A binary classification of dieback and nondieback was used to

create the prediction map. The difference values for known dieback areas that were within ± 1 S.D. of the $\bar{x}$ difference value were classified as dieback. A test of independence (G) and an index of association ($\gamma$) were used to compare the verification data against the dieback prediction map.

## RESULTS

### Unsupervised classification approach

The prediction maps generated using the unsupervised classification approach accurately predicted the distribution of dieback and nondieback at approximately 70 percent of the verification sites. The goodness-of-fit data for the TM spectral classes created from the transformed and untransformed imagery indicated that the observed pixel frequencies for some classes falling within the dieback areas were significantly higher than their frequencies in nondieback areas within the buffer zone ($G^2 > 1100$ for all images, d.f. > 50). The prediction maps for both unsupervised classifications were positively associated ($P < 0.05$ for G and positive $\gamma$) with the verification data (Tables 2a and 2b). The prediction accuracy of the transformed image was only slightly better than the untransformed image (71.9 percent verses 68.8 percent).

Area estimates of both the transformed and untransformed data for dieback were 4343 ha (ca. 30 percent of the area) and for nondieback were 10,030 ha of the area (Figure 3). The majority of the predicted dieback areas were distributed along the east slope of the valley and the playa bottom. Some scattered areas of dieback were also predicted on the west slope of the valley.

### Change detection approach

The MSS mean difference values of both dieback and nondieback areas for the pre-dieback period from 1975 to 1979 were similar to the index value of 127, suggesting no change in IR reflectance during this period (Table 3 and Figure 4). The mean difference value for dieback areas was 128.8 and nondieback was 129.6. Because the dieback and nondieback values are similar to the neutral index value of 127, this suggests that no environmental change between 1975 and 1979 occurred that significantly influenced IR reflectivity. It also indicates that there were minimal differences in IR reflectivity between areas of dieback and nondieback prior to the dieback event.

In contrast, the mean difference values of dieback and nondieback areas for the post-dieback period from 1979 to 1988 were substantially lower than 127 (dieback, 100.5 and nondieback, 110.3) (Table 3 and Figure 5). This indicates that the brightness values for the 1988 image were darker within both dieback and nondieback areas. Because a significant reflectivity reduction was observed in both areas, the reduction could be related to calibration differences between MSS sensors or large scale environmental differences such as surface soil moisture or vegetation composition. However, the difference values for the dieback areas were significantly darker than for nondieback areas, suggesting an additional spectral influence associated with areas of dieback. Table 3 and Figure 5 show that the IR brightness

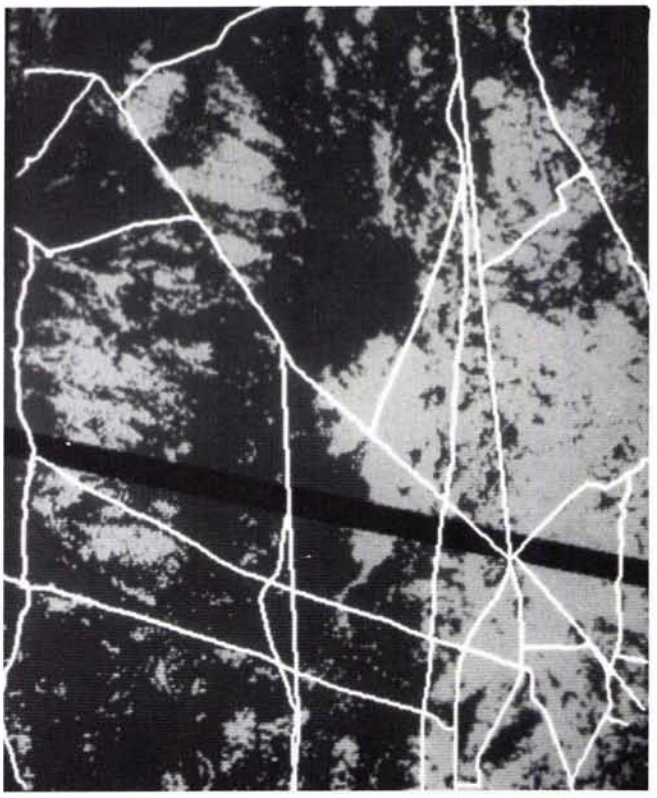

FIG. 3. Prediction map of the Puddle Valley study area showing dieback areas in light gray and nondieback areas in black. The map was produced from an unsupervised classification of TM transformed data. White lines are roads traversing the study area and the wide black diagonal strip crossing the map is where 18 bad lines of the image were deleted from the original TM data.

TABLE 2. ACCURACY ASSESSMENT OF PREDICTION MAPS CREATED FROM THE UNSUPERVISED CLASSIFICATION OF THE TRANSFORMED AND UNTRANSFORMED TM DATA AND CHANGE DETECTION USING MSS IMAGERY. INCLUDED IN THE TABLE ARE THE ASSOCIATED LIKELIHOOD RATIO CHI-SQUARE OF INDEPENDENCE (G), THE PROBABILITY OF A SMALLER G (P), THE GOODMAN-KRUSKAL $\gamma$ INDEX OF ASSOCIATION, AND THE ESTIMATED ACCURACY OF EACH PREDICTION MAP.

| Observed Category | Predicted Categories: Dieback | Nondieback | G | P | $\gamma$ |
|---|---|---|---|---|---|
| (a) Untransformed Thematic Mapper data - unsupervised classification | | | | | |
| **Dieback** | 12 | 18 | | | |
| **Nondieback** | 12 | 54 | 5.24 | 0.02 | 0.50 |
| Estimated accuracy 66/96 = 68.8% | | | | | |
| (b) Transformed Thematic Mapper data - unsupervised classification | | | | | |
| **Dieback** | 12 | 17 | | | |
| **Nondieback** | 8 | 52 | 8.83 | 0.003 | 0.64 |
| Estimated accuracy 64/89 = 71.9% | | | | | |
| (c) 1979 minus 1988 Multispectral Scanner data - change detection image | | | | | |
| **Dieback** | 17 | 10 | | | |
| **Nondieback** | 39 | 29 | 0.25 | 0.62 | 0.12 |
| Estimated accuracy 46/95 = 48.4% | | | | | |

TABLE 3. STATISTICS FOR DIEBACK AND NONDIEBACK AREAS THAT WERE GENERATED FROM DIFFERENCE VALUES DERIVED BY SUBTRACTING THE BRIGHTNESS VALUES OF TWO MSS BAND 6 (0.7 TO 0.8μM) IMAGES. A STUDENT'S T-VALUE WAS USED TO DETERMINE WHETHER AREAS OF DIEBACK AND NONDIEBACK WERE SIGNIFICANTLY DIFFERENT.

| Observed Category | Mean Difference Values | SD | t | d.f. |
|---|---|---|---|---|
| (a) 1979 *minus* 1975 image | | | | |
| Dieback areas | 128.8 | 11.7 | *** | *** |
| Nondieback areas | 129.6 | 8.0 | 2.76 | 25,118 |
| (b) 1988 *minus* 1979 image | | | | |
| Dieback areas | 100.5 | 6.6 | *** | *** |
| Nondieback areas | 110.3 | 9.4 | 46.60 | 25,118 |

values in the 1988 image averaged 9.8 values lower in dieback areas than in nondieback areas.

However, when the 1979/1988 difference map was compared to the verification sites, the areas of predicted change agreed with the verification data only 48.4 percent of the time. Table 2c shows that the change detection approach consistently overestimated dieback. The G-statistic did not differ significantly from zero; therefore, the change detection map was not significantly better at representing dieback distribution than a random classification of pixels.

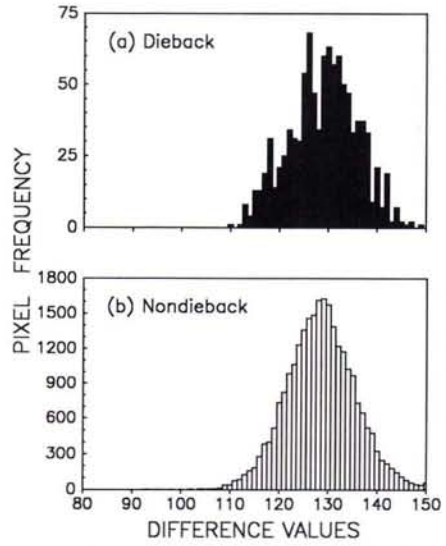


FIG. 4. Histogram of near infrared (0.7 to 0.8μm) difference values for known dieback ($x$ = 128.8, SD = 11.7) and nondieback ($x$ = 129.6, SD = 8.0) areas on the change detection image created by subtracting values of the 1975 MSS image from the 1979 MSS image. The two images were selected to represent the pre-dieback period.

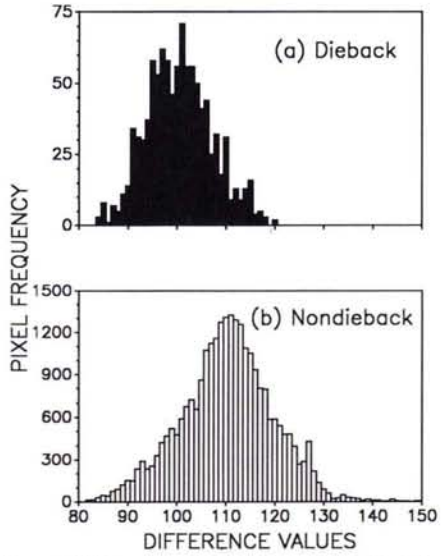


FIG. 5. Histogram of near infrared (0.7 to 0.8μm) difference values for known dieback ($x$ = 100.5, SD = 6.6) and nondieback ($x$ = 110.3, SD = 9.4) areas on the change detection image created by subtracting values of the 1979 MSS image from the 1988 MSS image. The 1979 image is pre-dieback and the 1988 image is post- dieback.

## DISCUSSION

One might conclude that the unsupervised approach was successful because of its classification accuracy of greater than 70 percent. However, there is still uncertainty over what actually influenced the classification results produced by the unsupervised and change detection approaches. The unsupervised approach clusters similar spectral reflectance patterns that are influenced by the interaction of electromagnetic energy with Earth surface features, the atmosphere, and the remote sensing system. Vegetation in a semiarid environment is sparsely distributed; even healthy stands of shrubs in salt-desert shrub communities have less than 25 percent cover with interspaces among shrubs rarely vegetated except for microphytic crusts (West, 1983). An unsupervised classification integrates spectral reflectance that is influenced by soils, shadow, plant components, and litter. Considering these influencing factors, it is doubtful whether the derivation of many, if any, spectral classes was directly affected by shrub mortality. A more probable explanation is that the environments most prone to shrub dieback are spectrally unique. If this is true, plant community ecologists might learn more about shadscale habitat characteristics and mortality differences by studying dieback and nondieback areas discriminated through analysis of remotely sensing data.

In contrast to the unsupervised approach, the results from the change detection approach might be considered much less successful. However, the results may provide additional insight related to exotic annual weed invasion patterns in the Great Basin. Data presented in Table 3 and Figure 5 indicate that, after the dieback event began, pixels in areas of known dieback averaged 9.8 brightness values lower than for similar areas of nondieback. Yet, the agreement between the change detection map and the field verification data was only 48.4 percent. The most obvious explanation for these results is that the change detection approach was sensitive to environmental change irrespective of dieback. It was noted in the field that the ground surface in most dieback areas was darkened by litter produced from exotic annual forbs from the preceding year (Figure 6). The vegetation data collected in Puddle Valley by Dobrowolski and Ewing (1990) also showed that increased concentrations of exotic annual weeds were often associated with areas of dieback. However, because both of our studies began after the

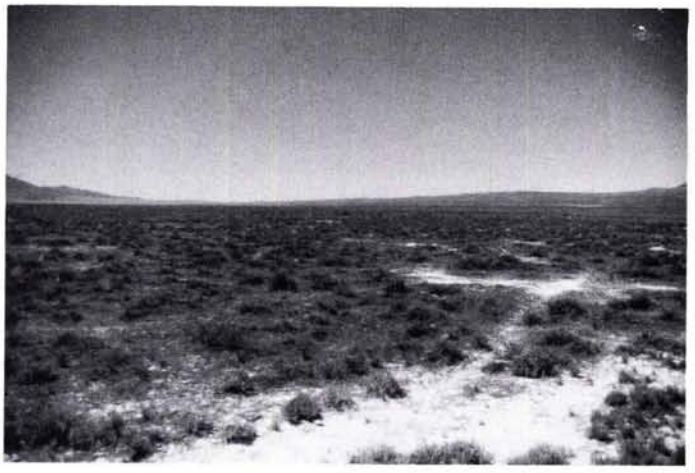

FIG. 6. A picture of a large dieback area. In the dieback area the surface of the ground is darkened by annual weed litter remaining from the previous 1987 growing season. There are live shrubs within the light area located at the bottom central portion of the picture.

initial dieback event, it is difficult to determine whether annual weeds invaded prior to, or after dieback. A display of multitemporal color composite images (Plate 1) shows the pre- and post-dieback results. The "after dieback" image shows red patterns indicating significantly lower IR reflectance in 1988. These patterns are obviously related to changes on the ground that could only be caused by variations in soil moisture or vegetation.

It is probable that not all areas experiencing increases in annual weeds also experience shrub dieback. The low correlation between the change detection map and verification data indicates that not all darker areas experienced dieback. Assuming litter is the factor influencing the reduction of IR in 1988, then change detection results indicate there were areas invaded by annuals where dieback was not prevalent.

Another possible explanation for low correlation between the change detection approach and the field verified data is that the binary classification scheme imposed upon the field verification data did not account for varying degrees of shrub mortality. Based upon the classification criterion that 95 percent must be dead, some areas with significant shrub mortality (i.e., 85 percent) may not have been classified as dieback. This explanation is supported by the error matrix in Table 2c that shows approximately three out of four misclassifications resulted because dieback was predicted, but the verification data indicated nondieback.

Aside from demonstrating the general capabilities of satellite data for monitoring shrub dieback in semiarid communities, this research also demonstrated the application of two statistical techniques, the goodness-of-fit tests and Goodman and Kruskal gamma. The goodness-of-fit tests provided a nonbiased criterion for selecting spectral classes associated with dieback. Typically, in analyses of remotely sensed data, such decisions are

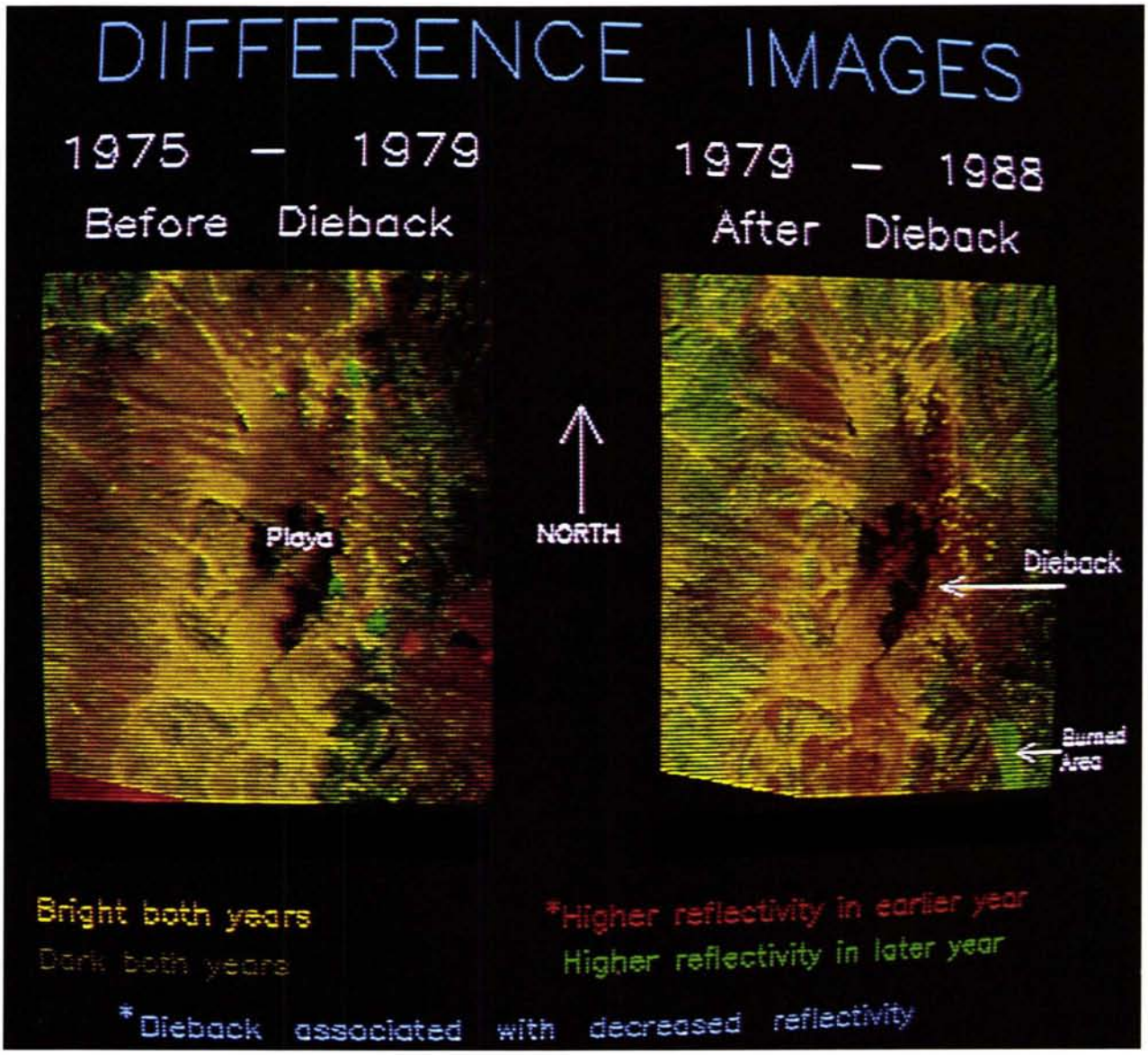


PLATE 1. Difference images of the study area before and after dieback. The images were photographed from a high resolution RGB display monitor. The images were created by assigning the red color plane of the display to MSS band 6 (NIR) of the earlier image and the green color plane to the same band of the later image. Areas with red hues indicate the location was brighter in the earlier image, green areas were darker in the earlier image, yellow areas were light in both images, and brown areas were dark in both images. Notice that after dieback there is a significant increase of red distributed around the playa area and other areas throughout the image which indicates these areas were darker in 1988 than they were in 1979.

subjectively made by the observer and thus are potentially non-replicable. $\gamma$ provided a useful index of the strength of associations between predictions and field observations of dieback and nondieback.

The results also indicated that little improvement in mapping accuracy was achieved by using the Tasseled Cap transformed versus untransformed data. This is probably due to the influence of soils, as explained by Tueller and Oleson (1989) who also worked in a Great Basin shrub environment. Huete and Jackson (1987) report that on arid rangelands, soil and litter greatly influenced the Greenness component derived by the Tasseled Cap transformation. The transformed results of this study may have improved if study area reflectance data were used to produce site-specific transformation coefficients as described by Huete *et al.* (1984) and Ezra *et al.* (1984). For practical purposes, additional vegetation indices were not evaluated. However, the Soil-Adjusted Vegetation Index (SAVI) (Huete, 1988) is a transformation recently developed specifically for arid/semiarid environments that should be evaluated in future studies.

Remote sensing of vegetation dynamics has previously concentrated on abrupt changes in community structure such as deforestation and desertification. However, this study suggests that satellite images can detect subtler changes in semiarid vegetation communities. Given these results, it appears that digital satellite data could be useful for monitoring vegetation change in semiarid environments at a regional scale.

In preparing for this study, the advantages of satellite data for large-area monitoring became apparent. Digital images are available with world-wide coverage for different seasons over many years, in contrast to the limited global availability of aerial photography, which has been used most often to detect forest dieback (Ciesla, 1989). Such availability allows images to be selected at the optimal time for vegetation monitoring, a factor critical for identifying plant communities of the Great Basin (Price *et al.*, 1985) and likely to be important in other semiarid regions.

## ACKNOWLEDGMENTS

We thank D. Verbayla for assistance in data collection and analysis; D. Ramsey for assistance in data analysis; and J. MacMahon, T. Slocum, M. Jakubauskas, S. Egbert, and anonymous reviewers for critical review of the manuscript. Research was funded by Environmental Protection Agency grant CR-814317-01-0, Utah Agricultural Experiment Station Project P-771. This study represents a cooperative effort among the Ecology Center, Department of Range Science, and Department of Geography and Earth Resources at Utah State University.

## REFERENCES

Bauer, M. C., J. E. Cipra, P. E. Anuta, and J. E. Etheridge, 1979. Identification and area estimation of agricultural crops by computer classification of Landsat MSS data. *Remote Sensing of Environment,* 9:77–92.

Blaisdell, J. A., and R. C. Holmgren, 1984. *Managing Intermountain Rangelands — Salt Desert Shrub Ranges.* U.S.D.A. Forest Service, General Technical Report, INT-163. Ogden, Utah.

Campbell, J. B., 1987. *Introduction to Remote Sensing.* Guilford Press, New York, N.Y.

Carneggie, D. M., B. S. Schrumpf, and D. A. Mouat, 1983. Rangeland Applications. *The Manual for Remote Sensing, Vol.* 2 (R. N. Colwell, editor), The American Society of Photogrammetry and Remote Sensing, Falls Church, Virginia, pp. 2325–2384.

Chavez, P. S., 1975. Atmospheric, solar, and M.T.F. corrections for ERTS digital imagery. *Proceedings of the American Society of Photogrammetry,* pp. 69–69a.

Ciesla, W. M., 1989. Aerial photos for assessment of forest decline — a multinational overview. *Journal of Forestry,* 87:37–41.

Crist, E. P., and R. C. Cicone, 1984. A physically-based transformation of Thematic Mapper data — The TM tasseled cap. *IEEE Transactions on Geoscience and Remote Sensing,* GE-22:256–263.

Dobrowolski, J. P., and K. Ewing, 1990. Vegetation dynamics and environmental attributes of a Great Basin valley exhibiting widespread shrub dieback. *Proceedings — Symposium on Cheatgrass Invasion, Shrub Die-off, and Other Aspects of Shrub Biology and Management.* USDA Forest Service, General Technical Report, INT-276. pp. 103–114.

Ezra, C. E., L. R. Tinney, and R. D. Jackson, 1984. Consideration for implementing vegetation indices for agricultural applications. *Technical Papers, 50th Annual Meeting of the American Society of Photogrammetry,* pp. 526–536.

Hoffer, R. M., 1984. Remote sensing to measure the distribution and structure of vegetation. *The Role of Terrestrial Vegetation in the Global Carbon Cycle: Measurement by Remote Sensing, SCOPE* 23. (G. M. Woodwell, editor). Wiley, New York, pp. 131–159.

Huete, A. R., 1988. A Soil-Adjusted Vegetation Index (SAVI). *Remote Sensing of Environment,* 25:295–309.

Huete, A. R., and R. D. Jackson, 1987. Suitability of spectral indices for evaluating vegetation characteristics on arid rangelands. *Remote Sensing of Environment,* 23:213–232.

Huete, A. R., D. F. Post, and R. D. Jackson, 1984. Soil spectral effects on 4-space vegetation discrimination. *Remote Sensing of Environment,* 14:155–165.

Iverson, L. R., and P. G. Risser, 1987. Analyzing long-term changes in vegetation with geographic information system and remotely sensed data. *Adv. Space Res.,* 7:183–194.

Jakubauskas, M. E., K. P. Lulla, and P. W. Mausel, 1990. Assessment of vegetation change in a fire altered forest landscape. *Photogrammetric Engineering & Remote Sensing,* 56:371–377.

Jensen, J. R., 1986. *Introductory Digital Image Processing: A Remote Sensing Perspective.* Prentice-Hall, Englewood Cliffs, New Jersey, 379 p.

Kauth, R. J., and G. S. Thomas, 1976. The Tasseled Cap—A graphic description of the spectral-temporal development of agricultural crops as seen by Landsat. *Proceedings, Symposium on Machine Processing of Remotely Sensed Data. Laboratory for the Applications of Remote Sensing,* pp. 41–51.

Liebetrau, A. M., 1983. *Measures of Association.* Sage Publications, Newbury Park, California.

Lowell, K. E. and J. H. Astroth, Jr. 1989. Vegetative succession and controlled fire in a glades ecosystem. *International Journal of Geographical Information Systems,* 3:69–81.

Mann, H. S., K. A. Shankaranarayan, and R. P. Dhir, 1984. Natural resource survey and environmental monitoring in arid-Rajasthan using remote sensing. *Deserts and Arid Lands* (F. El-Baz, editor). Martinus Nijhoff, Boston, Massachusetts, pp. 157–170.

Maxwell, E. L., 1976. Multivariate system analysis of multispectral imagery. *Photogrammetric Engineering & Remote Sensing,* 42:1173–1186.

McGraw, J. F., and P. T. Tueller, 1983. Landsat computer-aided analysis techniques for range vegetation mapping. *Journal of Range Management,* 36:627–631.

Mueller-Dombois, D., 1984. Classification and mapping of plant communities: a review with emphasis on tropical vegetation. PMMA*The Role of Terrestrial Vegetation in the Global Carbon Cycle: Measurement by Remote Sensing, SCOPE* 23 (G. M. Woodwell, editor). Wiley, New York, pp. 21–90.

NASA, 1988. *Earth System Science: A Closer View, A Program for Global Change.* University Corporation for Atmospheric Research, Boulder, Colorado. 208 p.

Nelson, D. L., K. T. Harper, K. C. Boyer, D. J. Weber, B. A. Haws, and J. R. Marble, 1989. Wildland shrub dieoffs in Utah: an approach to understanding the cause. *Proceedings — Symposium on Shrub Ecophysiology and Biotechnology* (A. Wallace, E. D. McArthur, and M. R. Haferkamp, compilers), 30 June - 2 July 1987; Logan, Utah, U. S. Department of Agriculture, Forest Service. General Technical Report INT- 256. Ogden, Utah, pp. 119–135.

Pilon, P. G., P. J. Howarth, and R. A. Bullock, 1988. An enhanced classification approach to change detection in semi-arid environments. *Photogrammetric Engineering & Remote Sensing,* 54:1709–1716.

Price, K. P., M. K. Ridd, and J. A. Merola, 1985. An integrated Landsat/

ancillary data classification of desert rangeland. *Technical Papers, 51st Annual Meeting of the American Society of Photogrammetry,* pp. 538–545.

Pyke, D. A. and J. P. Dobrowolski, 1989. Shrub dieback in the Great Basin. *Utah Science,* 50:66–73.

Rasool, S. I., 1985. On monitoring global change by satellites. *Global Change: The Proceedings of a Symposium Sponsored by the International Council of Scientific Unions (ICSU)* (T. F. Malone and J. G. Roederer, editors), 20th general assembly in Ottawa, Canada on September 25, 1984. Cambridge University Press, New York, pp. 429–439.

Robinove, C. J., P. S. Chavez, Jr., D. Gehring, and R. Holmgren, 1981. Arid land monitoring using Landsat albedo difference images. *Remote Sensing of Environment,* 11:133–156.

Rock, B. N., J. E. Vogelmann, D. L. Williams, A. F. Vogelmann, and T. Hoshizaki, 1986. Remote detection of forest damage. *BioScience,* 36:439–445.

Rohde, W. G., J. K. Lo, and R. A. Pohl, 1978. EROS data center Landsat digital enhancement techniques and imagery availability, 1977. *Canadian Journal of Remote Sensing,* 4:63–76.

Running, S. W., D. L. Peterson, M. A. Spanner, and K. B. Teuber, 1986. Remote sensing of coniferous forest leaf area. *Ecology,* 67:273–276.

Sader, S. A., 1987. Digital image classification approach for estimating forest clearing and regrowth rates and trends. *Proceeding of IGARSS '87 Symposium,* Ann Arbor, pp. 209–213.

SAS Institute Inc. 1988. *SAS/STAT Users Guide, Release 6.03 Edition.* SAS Institute, Cary, North Carolina.

Sokal, R. R. and F. J. Rohlf, 1981. *Biometry, 2nd edition.* Freeman and Company, New York.

Tueller, P. T. 1987. Remote sensing science applications in arid environments. *Remote Sensing of Environment* 23:143–154.

Tueller, P. T., and S. G. Oleson, 1989. Diurnal radiance and shadow fluctuations in the cold desert shrub plant community. *Remote Sensing of Environment,* 29:1–13.

Tucker, C. J., 1979. Red and photographic infrared linear combinations for monitoring vegetation. *Remote Sensing of Environment,* 8:127–150.

Tucker, C. J., J. R. G. Townshend, and T. E. Goff, 1985. African land-cover classification using satellite data. *Science,* 227:369–375.

Vogelmann, J. E., and B. N. Rock, 1988. Assessing forest decline in high-elevation coniferous forests in Vermont and New Hampshire using Thematic Mapper data. *Remote Sensing of Environment,* 24:227–246.

Walker, K., and C. Zenone, 1988. Multitemporal Landsat Multispectral Scanner and Thematic Mapper data of the Hubbard Glacier region, southeast Alaska. *Photogrammetric Engineering & Remote Sensing,* 54:373–376.

West, N.E., 1983. Intermountain salt-desert shrubland. *Temperate Deserts and Semi-Deserts, Vol. 5, Ecosystems of the World* (N. E. West editor). Elsevier, Amsterdam, pp. 375–397.

Wiegand, C. L., A. J. Richardson, and E. T. Kanemasu, 1979. Leaf area index estimates for wheat from Landsat and their implications for evapotranspiration and crop modeling. *Agronomy Journal,* 71:336–342.

Wilson, R. O., and P. T. Tueller. 1987. Aerial and ground spectral characteristics of rangeland plant communities in Nevada. *Remote Sensing of Environment,* 23:177–191.

Woodwell, G. M., J. E. Hobbie, R. A. Houghton, J. M. Melillo, B. Moore, A. B. Park, B. J. Peterson, and G. R. Shaver, 1984. Measurement of changes in the vegetation of the earth by satellite imagery. *The Role of Terrestrial Vegetation in the Global Carbon Cycle: Measurement by Remote Sensing, SCOPE* 23 (G. M. Woodwell, editor). Wiley, New York, pp. 221–240.

Woodwell, G. M., R. A. Houghton, T. A. Stone, R. F. Nelson, and W. Kovalick, 1987. Deforestation in the tropics - New measurements in the Amazon Basin using Landsat and NOAA advanced very high-resolution radiometer imagery. *Journal of Geophysical Research,* 92D:2157–2163.

(Received 13 June 1990; revised and accepted 24 June 1991)

## Forthcoming Articles

*Paul V. Bolstad* and *T. M. Lillesand,* Rule-Based Classification Models: Flexible Integration of Satellite Imagery and Thematic Spatial Data.

*Pat S. Chavez, Jr.,* Comparison of Spatial Variability in Visible and Near-Infrared Spectral Images.

*Liang-Chien Chen* and *Liang-Hwei Lee,* Progressive Generation of Control Frameworks for Image Registration.

*John Crews,* Overplotting Digital Geographic Data onto Existing Maps.

*Claude R. Duguay* and *Ellsworth F. LeDrew,* Estimating Surface Reflectance and Albedo from Landsat-5 Thematic Mapper over Rugged Terrain.

*Jeffery C. Eidenshink,* The 1990 Conterminous U. S. AVHRR Data Set.

*G. M.Foody, N. A. Campbell, N. M. Trodd,* and *T. F. Wood,* Derivation and Applications of Probabilistic Measures of Class Membership from the Maximum-Likelihood Classification.

*Clive S. Fraser* and *James A. Mallison,* Dimensional Characterization of a Large Aircraft Structure by Photogrammetry.

*Clive S. Fraser* and *Mark R. Shortis,* Variation of Distortion within the Photographic Field.

*Dennis L. Helder, Bruce K. Quirk,* and *Joy J. Hood,* A Technique for the Reduction of Banding in Landsat Thematic Mapper Images.

*Wei Ji, Daniel L. Civco,* and *William C. Kennard,* Satellite Remote Bathymetry: A New Mechanism for Modeling.

*David P. Lanter* and *Howard Veregin,* A Research Paradigm for Propagating Error in Layer-Based GIS.

*Jay Lee, Peter F. Fisher,* and *Peter K. Snyder,* Modeling the Effect of Data Errors in Digital Elevation Models on Feature Extraction.

*John Grimson Lyon, Ross S. Lunetta,* and *Donald C. Williams,* Airborne Multispectral Scanner Data for Evaluating Bottom Sediment Types and Water Depths of the St. Marys River Michigan.

*John Grimson Lyon* and *Richard G. Greene,* Use of Aerial Photographs to Measure Historical Areal Extent of Lake Erie Coastal Wetlands.

*J. Olaleye* and *W. Faig,* Reducing the Registration Time for Photographs with Non-Intersecting Crossarm Fiducials on the Analytical Plotter.

*Albert J. Peters, Bradley C. Reed,* and *Donald C. Rundquist,* A Technique for Processing NOAA-AVHRR Data into a Geographically Referenced Image Map.

*Benoit Rivard* and *Raymond E. Arvidson,* Utility of Imaging Spectrometry for Lithologic Mapping in Greenland.

*Kathryn Connors Sasowsky, Gary W. Petersen,* and *Barry M. Evans,* Accuracy of SPOT Digital Elevation Model and Derivatives: Utility for Alaska's North Slope.

*Vittala K. Shettigara,* A Generalized Component Substitution Technique for Spatial Enhancement of Multispectral Images Using a Higher Resolution Data Set.

*Michael B. Smith* and *Mitja Brilly,* Automated Grid Element Ordering for GIS-Based Overland Flow Modeling.

*David M. Stoms, Frank W. Davis,* and *Christopher B. Cogan,* Sensitivity of Wildlife Habitat Models to Uncertainties in GIS Data.

*Khagendra Thapa* and *John Bossler,* Accuracy of Spatial Data Used in Geographic Information Systems.